

High-Power Microwave Generation With Photoconductors

Oved S. F. Zucker, *Member, IEEE*

(Invited Paper)

Abstract—This paper describes an unconventional method for the generation of high-power microwave (HPM) with orders of magnitude higher in power and energy than competing concepts. The method brings together several synergistic concepts. First, microwaves are synthesized cycle by cycle (digital synthesis) by the discharge of charged transmission lines. The method presented here generates a bipolar pulse with substantial impedance transformation. Second, photonic *on* switching via photoconductors is used to provide coherent timing. Third, the generation of HPM at extremely low impedance takes advantage of a fortuitous match between the peak Poynting power associated with thin films and high current density related to very high carrier concentration in photoconductors. Finally, unique HPM circuitry, termed a Switch Bypass Source circuit, is presented that affords multiple cycle generation and high pulse energy which avoids cascading switch losses. The combination of these techniques transforms HPM technology from the present level of gigawatts and hundreds of joules per pulse to levels that are orders of magnitude higher.

Index Terms—High-power microwave, high-power radiation, light activated silicon switch, microwave, photoconductivity, radio frequency, ultra-wideband.

I. INTRODUCTION

PHOTOCONDUCTIVE-BASED high-power microwave (HPM) technology originated with the realization that first, relativistic-beam-based HPM is limited in both maximum power (~ 10 GW), and lifetime due to electric field limit in the cavity and substantial cavity erosion. Secondly, the total energy and power required for various defense missions approach a MJ and a TW, respectively. It was realized that such large power and energy delivered from practical robust systems could be achieved by arraying multiple HPM sources utilizing many photoconductive switches that were controlled by a single coherent laser source.

The subject of photoconductivity is intimately connected with the photodiode, where light is used to create carriers (electrons and holes) in a semiconductor. While the photodiode current is proportional to the light intensity, the photoconductor (PC) is a switch where a short pulse of light is used to transition the device from blocking to conducting. In this paper we are interested

in photoconductors operating in the sub nanosecond switching speed with individual switching powers above a MW. This is the regime of interest for the generation of HPM.

A good switch is one which reverts from insulator to conductor in a short time compared to the relevant circuit time constant. Further, we desire a low *on* resistance, and a high *off* resistance to minimize losses during both blocking and conducting. Lastly, we desire to minimize conduction onset jitter to provide simultaneity between disparate switches. Pulsed laser light is the preferred light source to affect turn on because i) its narrow pulse width provides an arbitrarily short switching speed; ii) it is capable of synchronizing many switches simultaneously and thereby provides coherence between the various generated electrical pulses; and iii) its photon energy can match the semiconductor's band gap to provide efficient carrier generation.

The two types of switching processes in semiconductors are commonly termed linear and nonlinear. The latter is distinguished from the former by the use of avalanche in the semiconductor to create most of the carriers needed for conduction, while the former uses only photon-generated carriers. Two semiconductor device structures commonly used are bulk semiconductor material and back-biased junctions of various types such as the transistor and thyristor. Bulk devices rely on the high resistivity of the semiconductor to provide the *off* switching state, while junction devices rely on a depletion layer to provide the blocking. The bulk device has considerable leakage current in the blocking state and can therefore block for only short durations, while the junction device has many orders of magnitude lower leakage current and can thus block the current flow very efficiently compared to bulk devices. On the other hand, junction devices have inherent voltage limits associated with their background doping, typically ~ 10 kV, while a bulk device can be made as long as desired and in principle, if long enough, can hold any voltage. In practice the blocking voltage in bulk devices is only modestly higher than junction devices since other limitations, such as surface breakdown and reduced average blocking field, affect the performance of the device.

Historically, the initial development of photoconductive-based technology has taken two distinct routes by two independent teams without the knowledge of each other's work. One approach, led by D. Auston at Bell Laboratories, utilized bulk silicon for both the capacitive energy storage as well as the switch, with the switch operated in the linear regime and activated in the picosecond regime with a mode locked YAG laser [3], [6]. The second approach at the Lawrence Livermore

Manuscript received April 4, 2008; revised April 30, 2008. Current version published October 10, 2008.

The author is with Polarix Corporation, San Diego CA USA (e-mail: oved.zucker@polarixcorp.com).

Color versions of one or more of the figures in this paper are available online at <http://ieeexplore.ieee.org>.

Digital Object Identifier 10.1109/JLT.2008.925611

TABLE I
HISTORICAL EXPERIMENTAL RESULTS WITH PHOTOCONDUCTIVE SWITCHING BY THE LEADING TEAMS [1]–[9]

	Rise time, τ (ns)	Current, I (A)	Current Rate of Rise, $I\text{-dot}$ (kA/ μ s)	Power, P
Page, Roberts Westinghouse, 1974	150	3000	20	10 MW
Auston Bell Labs, 1975	0.01	0.3	30	4.5 W
Zucker, Long LLNL, 1975	13	10000	750	10 MW
Auston, LeFur Bell Labs, 1976	0.025	50	2000	45 kW
Long, Zucker LLNL, 1977	0.15	5000	10000	5 MW

National Laboratories (LLNL)/Westinghouse team (headed by the author of this paper), utilized silicon thyristor (junction) devices, termed LASS for Light Activated Silicon Switch [4], [5], [7]–[9]. These devices operated in the linear regime, with polyethylene thin film transmission lines (TLs) for energy storage. As shown in Table I, the differences in performance between these two approaches are the power and the current. These studies were an early demonstration of the superior power and current available when operating photoconductors in low-impedance circuits associated with dielectric thin films.

The first study of photoconductive switching occurred in 1974 at Westinghouse by Page and his coworkers using high voltage Si thyristors and YAG lasers [1], [2]. Silicon was chosen as the material due to its premier performance as a power device. YAG laser light was utilized due to its wavelength match to the band gap of Si. Further, the penetration depth for YAG light into Si is around a millimeter, which in turn is the typical device thickness for multi-kilovolt thyristors. They achieved a current rate of rise, $I\text{-dot}$, of 20 kA/ μ s [1]. In 1975, Auston's team at Bell Laboratories achieved picosecond switching with 4.5 W of power, followed a year later by an improvement to 45 kW at an $I\text{-dot}$ of 2 MA/ μ s [3], [6]. At the same time, the author of this paper was performing similar experiments at LLNL and achieved nanosecond switching time at a much higher current and power (megawatt) level [4]. Two years later, the author's team achieved rise times of 150 ps with an $I\text{-dot}$ of 10 MA/ μ s at 5 MW of power [9].

In the 1980s, devices based on the avalanche process were explored to reduce the amount of light required in various semiconductors in both the bulk and the junction configurations. Avalanche in semiconductors is a well-known phenomenon and causes no damage provided current densities remain low. With avalanche gain of a thousand or more, a pulsed laser diode could activate a small semiconductor switch at up to a MW switching power. Since laser diodes are in the 890 nm wavelength range, a GaAs switch was chosen as the most suitable material. Since GaAs junctions are low in voltage, the voltage was raised by using bulk GaAs which can be arbitrarily long and thus block a higher voltage. Thus was born the bulk avalanche semiconductor switch, or BASS, which was introduced by Power Spectra, Inc. Avalanche designs were explored with III-V materials such as GaAs and InP as well as Si, diamond, and SiC by various investigators [10]–[12]. This approach, however, does not lend itself to practical HPM

applications due to a combination of limitations that include low current, high forward voltage drop, high leakage current, poor ohmic contacts, and/or the lack of a matching laser.

At the same time that many investigators focused on GaAs avalanche technology, the author continued to focus on high current linear junction Si switches. While considerable investigation has been devoted to these other approaches [10]–[15], none have reached the level of performance in comparison to the back-biased junction silicon devices linearly activated with a 1.06 μ m YAG laser. The author proposed utilizing thin dielectric films with junction Si photoconductors in various switching systems. Thin film dielectric TLs have inherently much higher breakdown fields that are useful for high-power applications. The use of a back-biased junction has the added advantage of very low leakage current which results in a more practical switch without any voltage penalty in the low-impedance regime, and further, the linear regime affords a very low *on* resistance needed for operating many switches in series to extend the pulse length and thus the pulse energy [4], [8], [9], [16].

In 1985, a paper on a land-based terawatt system was included in the DOD HPM conference [17]. A patent for the system was applied for in 1986 and was put under the secrecy act until 1992 [18]. The approach and the patent described a TW array of individual sources utilizing the integration of thin films with junction photoconductors, and pulse train generation with sequential switching.

In this paper, we discuss HPM generation with linear silicon junction PCs. High-speed low-impedance circuits can only be realized in thin film transmission lines. A family of thin-film-based circuits with linear Si switches will be discussed for the first time, which provides a pathway to high-power, high-speed HPM systems with some advantages.

II. THEORETICAL BACKGROUND

A. Theoretical Considerations for Thin-Film-Based HPM

By its nature, HPM consists of both high-power and microwave frequencies. Digital synthesis is the process where the individual cycles are created half cycle by half cycle through the discharge of charged TLs. Thus, the switch must have a faster turn on time compared to the line's discharge time. For microwave generation, this time is below 100 ps.

The system in Fig. 1 shows a planar TL separated in the middle by a switch that extends over the full TL width, w . The

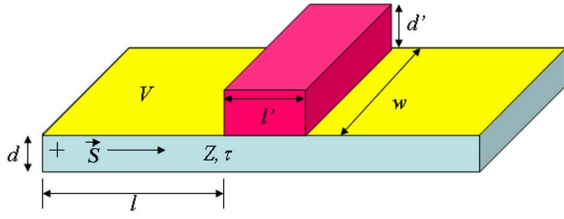


Fig. 1. Photoconductive switch with height, d' , and length, l' , attached to TEM transmission line with plate separation d and impedance Z . The switch and the TL have a width w .

switch width equals the line width in order to provide the fastest possible discharge and hence the highest power. This can be seen by imagining a switch that is much narrower than w situated in the middle of the line. Such a switch will force the current to narrowly channel through it, causing both a mismatch, which lengthens the pulse and reduces the power, and additional inductance that will limit the risetime. Similar arguments can be made for a switch much wider than w . The switch length l' is determined by the semiconductor blocking field, E_b , and the charge voltage, V . Likewise, the TL separation, d , is determined by its dielectric breakdown field, E_d , and the voltage, V .

Flooding the semiconductor with laser light transforms the switch from insulator to conductor, which switches the charged line on the left in Fig. 1 into the semi-infinite matched uncharged line on the right, i.e., the load. The initial line discharges into the second TL after switching in a double transit time, 2τ , where τ is the charged line length time. The resulting TEM wave travels in the direction of the Poynting vector, S , which is uniform over the TL cross sectional area. The Poynting vector can be written as:

$$\vec{S} = \vec{E}_d^2 / (4Z) \quad (1)$$

where Z is the wave impedance and E_d is the TL electric field. The total power can be calculated from the area and the average power density per unit area

$$P = (\vec{E}_d^2 / 4Z)(d \cdot w) \quad (2)$$

where d is the TL separation and w is the width of the plates. Typically, w is much larger than d and can be chosen as a linear scaling factor, as it does not affect the field limits

$$P/w = \vec{S} \cdot d. \quad (3)$$

Thus, for any given E-field, d determines the power per unit width the TL can deliver. In reality the breakdown electric field of the TL dielectric is a strong function of this TL thickness, d . Therefore, the thickness of the dielectric plays a key role in the overall performance of the HPM system.

B. Dependence of Electric Field Breakdown on Dielectric Thickness

The study of electric field breakdown is very broad. The two overriding factors that can characterize this phenomenon are first, the intrinsic field strength of the dielectric material and second, failure due to imperfections inherent in real structures.

To a first approximation, the intrinsic field strength is determined by the bond strength of the atom and molecule of the dielectric medium. While imperfections exist throughout the volume of the dielectric, those at the dielectric/metal interface dominate the failure mechanism. First, at the dielectric/metal interface, the change in resistivity approaches twenty orders of magnitude which causes field enhancement due to curvature. This field enhancement will reduce the ability to hold off a given voltage. Secondly and more important, a failure at this interface has additional energy available since charge flows from the adjacent metal electrode into the failed region. Thus, the breakdown continues to propagate through the dielectric in avalanche fashion. It has been shown experimentally that all dielectrics exhibit drastically lower breakdown fields in bulk relative to thin films. Hence, high voltage capacitors use thin films in series rather than thicker dielectrics. J. C. Martin *et al.* have done extensive tests on the breakdown of solid dielectrics [20]. Data extending over many thicknesses of dielectrics, from capacitor films to high voltage cable to dielectric blocks, all converge on the following conclusions: i) breakdown dependence on the area of the insulator is rather weak; ii) dielectric thicknesses of a few mm or more yield a rather low voltage breakdown field of around 50 kV/cm; iii) the field strength increases as the dielectric thickness decreases. For example, for thicknesses on the order of one mil and below, the breakdown field is in the MV/cm range.

The general behavior of the breakdown can be expressed with the following equation:

$$E_b = E_0 e^{-\frac{d}{d_0}} + E_{\text{Bulk}} \quad (4)$$

where E_0 is the bond energy, d is the dielectric thickness, d_0 is an experimental constant, and E_{Bulk} is the bulk breakdown field. While the absolute values of E_0 , E_{Bulk} , and d_0 will vary among dielectrics, the behavior illustrated by (4) is quite representative of the behavior of breakdown in dielectric materials. Equation (4) is plotted in Fig. 2 with values of 20 MV/cm, 12 μm , and 50 kV/cm for E_0 , d_0 , and E_{Bulk} , respectively. These values have been chosen to agree with data associated with MOSFET gate oxide, high-energy storage capacitors thin films (Mylar, Kapton, etc.) and high voltage cables [20], [21]. The difference in the breakdown E-field between thin films, a few MV/cm, and bulk dielectrics, around 50 kV/cm, approaches two orders of magnitude. Accordingly, the difference in the Poynting vector approaches four orders.

We do recognize that the thin film has a small cross sectional area and thus one should really compare the power per unit width, (3), by substituting (4) and (2) into (3). As shown in Fig. 2, the power per unit width has its maximum at a small thickness, with thin films exhibiting two orders of magnitude enhancement over bulk material. While this peak varies for different materials, it nevertheless remains in the range of 10 to 50 μm , i.e., below a few mils. For example, a TL whose width is 1 cm and has a spacing of 50 μm will transmit as much as 100 MW. Therefore, in order to transmit and generate the highest power and at the lowest volume at any width, it is imperative that we operate in the thin film regime.

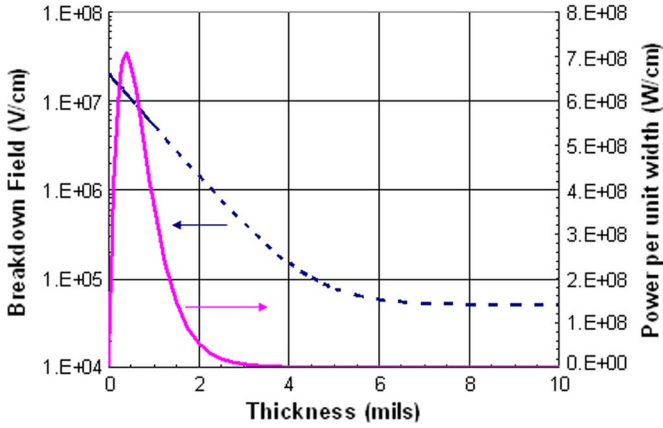


Fig. 2. Thickness dependence of breakdown field and power. Solid pink line: power per unit width at wave impedance in dielectric (Kapton) $Z = 200 \Omega$. Dashed blue line: electric breakdown field.

C. Switch Requirements

We intuitively recognize that regardless of the width, w , a small plate separation corresponds to low impedance. This corresponds to higher current which the switch has to carry. The current per unit width, H , in the TL above obeys the equation

$$H = I/w = E/2Z = Jd' \quad (5)$$

where J is the current density in the switch. With E in the MV/cm range and the wave impedance Z in the dielectric around 200Ω , we require the switch to carry around 5 kA/cm over the full width w . Risetime requirements restrict d' to be around a millimeter, which from (5) results in a requirement for J to be around 50 kA/cm^2 along its full width. The speed is dependent upon the switch height, d' , due to geometrical considerations and light transit time, as well as absorption length that limits the height to the millimeter range. For a detailed discussion, see Zucker *et al.* [22] Thus, we require a high current density that is achieved with minimal voltage drop.

In a semiconductor, the drift velocity of carriers will limit the current density:

$$J = nev_d \quad (6)$$

where n , e , and v_d are the carrier concentration, the electron charge, and the drift velocity, respectively. Under injection, saturation concentrations approach 10^{18} cm^{-3} and can reach 10^{20} cm^{-3} under laser illumination. If we choose a drift velocity that corresponds to an *on* state electric field of 1% of the blocking field, i.e., 1 kV/cm , we will have a 98% efficient switch. The corresponding v_d would thus be around 10^6 cm/s in Si leading to a current density of 160 kA/cm^2 .

This result is extremely important for high-power microwave applications. By comparing the current density required for a TL ($\sim 50 \text{ kA/cm}^2$) and the current density provided by semiconductors ($\sim 160 \text{ kA/cm}^2$), we see that the properties of these photoconductors allow for the integration of semiconductor switches into TLs that require a huge amount of power to be switched. These calculations show that with all carriers created

by photon absorption, a semiconductor can handle the linear current required by the most demanding TL power flow.

D. Transmission Line Loss Considerations

A parallel plate TL has resistive losses that must be taken into account. For a given frequency operation, as the separation distance decreases, the dissipation increases. More precisely, for a TL carrying an electromagnetic wave of frequency f , and whose length is one wavelength, the ratio of the power dissipated to the power entering the line is

$$P_d/P_0\lambda = 2\pi\delta/d \quad (7)$$

where δ is the penetration depth at frequency f into the TL plates and d is the plate separation. Thus, we see that with $d \sim 50 \mu\text{m}$, while the power can be very large the dissipation is also large. At frequency 1 GHz , the depth of penetration in copper is $2.1 \mu\text{m}$. Thus, approximately 10% of the power is dissipated along a one-wavelength-long TL. One consequence is that stringing lines together can be limiting either in length or in power. Another consequence is the need to transform to higher impedance as soon as possible. Circuits that perform both generation and transformation simultaneously are thus very important and will be discussed further below.

E. Material and Carrier Generation Considerations

The materials typically used for photoconductors include Si, GaAs, SiC, diamond, and other III-V and II-VI compound semiconductors. There are many key parameters when choosing which material is best suited for a specific application. First, while the blocking field increases with the semiconductor's bandgap, the availability of a laser whose wavelength matches that band gap is usually the limiting factor. Second, the carrier lifetime may be on the order of nanoseconds, leading to short devices with reduced voltages, requiring an increase of laser light intensity. Third, the maximum current density is limited by both the technology level of ohmic contacts to both p- and n-type materials as well as the carrier lifetime. Fourth, the resistance will be dependent on the mobility of both electrons and holes. Fifth, the maximum voltage will depend on the blocking field as well as the carrier lifetime which determines the length of the device. Finally, the thermal management will depend on the material's thermal conductivity, *on* voltage drop, and leakage in the *off* state.

While there are a number of candidates of interest for various reasons, from a systems point of view at present, Si is the overall winner. Si combines a very high current at low voltage drop, impressive mobility for both electrons and holes, a bandgap matched to pulsed YAG laser, a respectable thermal conductivity, and adequate blocking field.

Within Si, there are two main pathways to carrier generation: avalanche and linear activation. While avalanche activation requires less laser light, avalanche limits the current density by orders of magnitude and further results in much more *on*-state dissipation. Thus, for relatively low power microwave systems, avalanche switches may be adequate but for higher power systems, linear activation is superior. Furthermore, efficiency of diode laser pumping makes the energetic picture rather similar. For example, a 20% efficient diode pumped YAG uses $\sim 5 \text{ eV}$

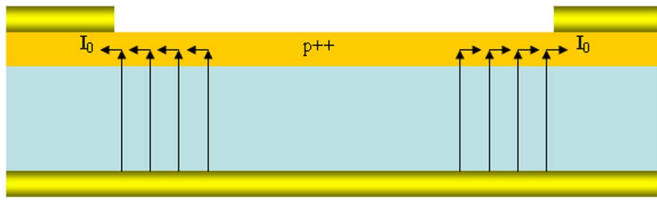


Fig. 3. Current flows only at the edges of the aperture. No current will flow in the middle of the device.

electrical energy to create an electron-hole pair. Avalanche uses 2–3 eV to create a carrier with electrical energy, but with considerable *on* resistance and inherently low current density and thus low power. Thus, the energy cost of a carrier, while a bit superior in the avalanche case, is not sufficient to justify using it. Overall, linear activation requires a few microjoules per MW of RF power generated [23] and thus makes the whole issue of laser energy moot.

A comparison of junctions versus bulk material is a focus on the impedance of operation. Bulk switches hold more voltage, but as the analysis has shown, higher power is realized only at low impedance with its comparatively lower voltage but much higher current which is right in the voltage range of junction devices. Thus, the added bonus of extremely lower leakage of junctions with their attendant lower *off* dissipation makes the junction PC the technology of choice.

F. Current Distribution and Light Access in the Semiconductor

Early optical apertures used in the LLNL/Westinghouse experiments [1], [2], [4], [5], [7]–[9] utilized etched holes (several millimeters in diameter) in the top electrode of the Si switches to provide light access. Experiments revealed that with this type of optical aperture, current did not flow either in the aperture or under the anode [1]. As seen in Fig. 3, current flow was restricted to the edges of the aperture. The problem with this aperture is that current from the electrode around the aperture has to reach the center of the aperture. Current from the center of the aperture to the edge, where the Ohmic contact to the electrode occurs, has to traverse the thin *p++* layer at the top. At high device current densities, the sheet resistance of this layer is too high to accommodate much current. Therefore, most of the semiconductor is unused and wasted.

In 1984, a company founded by the author, ECR, began to address some of these challenges associated with the integration of thin film dielectrics with junction silicon photoconductors. The work at ECR concentrated on simultaneously maximizing both the power and the rise-time. To achieve this goal, a new approach to coupling light into the system was created. Here, light is introduced through a beveled edge at an angle that allows light to cover the region between the electrodes, as seen in Fig. 4. More importantly, mounting the diode onto a gap in the transmission line at the bevel angle allows for a much higher field in the transmission line to gradually spread into the lower diode field with minimum field enhancement at the diode edge. This geometry led to much greater current and power handling capabilities by utilizing the entire volume of the semiconductor switch. With this geometry, ECR demonstrated 118 MW

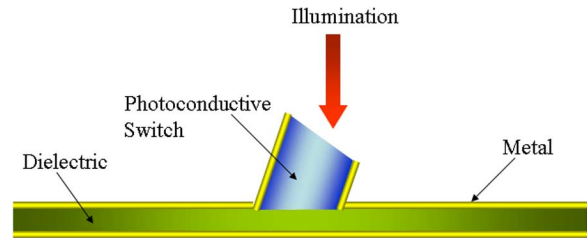


Fig. 4. TL with side illuminated switch.

switching with a rise-time of ~ 30 ps, with a corresponding current and current rise-time of 38 kA in $\sim 10^{15}$ A/s, as seen in Fig. 5. To this day, this *I*-dot record has not been surpassed by any other design [16], [24], [25].

The drawback to this configuration is that the switch bevel must now both hold the voltage and provide the aperture with the illumination light, which is rather difficult. The solution to this problem combines the top illumination from the Westinghouse aperture with the observation from Fig. 3. The top electrodes in Fig. 3 are moved closer together so that the spacing allows current to flow in the entire device. This can be established using a grid with separation in the $10 \mu\text{m}$ range and with Ohmic contacted bars in the few micrometer range. First developed by a Southern California company, OZI [26] and EG&G in the late 1990s, this design provides more than 80% light transparency and at the same time reduces the resistance (by reducing the conduction length) of the *p++* region sufficiently to carry the full current of the illuminated structure between the bars. This kind of transparent window can accommodate an average device current density of 50 kA/cm^2 and above. Beyond the obvious advantage of separating the voltage-holding region from the optical window region, an added feature of the grid was that now such a switch can be completely electrically shielded, as seen in Fig. 6. Thus, the switch can be electrically internal to a structure while still optically accessible from the outside. An electrically buried switch that still has optical access can now be the basis of a new circuit for the generation of many cycles. This is discussed in the appropriate section below.

III. CIRCUITS FOR HPM GENERATION

While the thin film TL switching method discussed above is the basis for achieving the highest power density possible, an actual HPM system has additional requirements which include: i) the generation of alternating-polarity pulse (i.e., no DC component); ii) generation of multiple, high-power cycles to extend the total pulse length and thus the energy by the HPM pulse; and iii) transformation to higher impedance, reducing conduction losses and assisting in impedance matching to a suitable radiator. In this section we discuss a number of novel circuits which achieve some or all of these requirements.

A. Utilizing Single Switch Circuitry

The simplest possible circuit for generation of HPM is shown in Fig. 7(a). A transmission line of temporal length τ and impedance Z_0 is switched into a matched load. For a transit time, $\tau = 0.5$ ns, the pulse frequency spectrum is shown in Fig. 7(b), containing frequencies from DC to well over

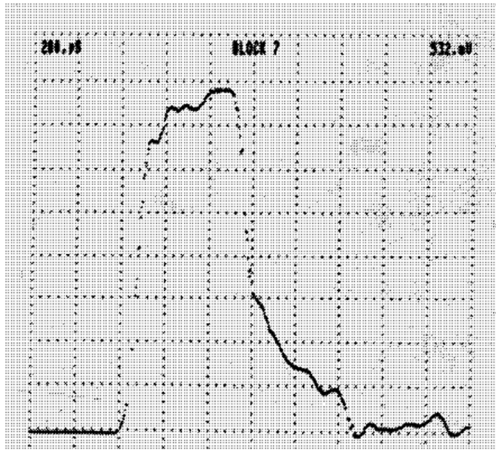


Fig. 5. 118 MW switching with 50 ps rise-time, $I \cdot \text{dot} = 10^{15}$ A/s.

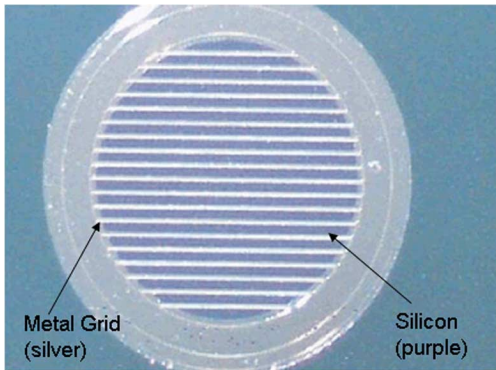


Fig. 6. Electrically shielded switch with optical access built by EG&G for OZI.

$f = 1/(2\tau)$. As τ becomes shorter and starts resembling an impulse, the spectrum width becomes more uniform, with the pulse energy distributed more uniformly. However, antennas of finite size do not radiate DC, and thus this type of generation would be radiated inefficiently. The ideal case for radiation applications is therefore a bipolar pulse generator. The smallest number of possible cycles for a generated wave is a single cycle. Such a pulse generator, shown in Fig. 8(a), confines its spectrum into a narrower bandwidth and thus will radiate more readily.

B. Utilizing Multiple Switch Circuitry

The thin film switched source, whether unipolar or bipolar, generates very high power in a small volume. Many such sources operated synchronously and in parallel can generate power up to the terawatt level. However, a single cycle limits the pulse energy—a Gigawatt over a nanosecond contains only a single Joule of energy. It is therefore judicious to generate pulse trains that contain many cycles without an appreciable reduction in pulse power due to cumulative dissipation.

The frozen wave circuit, invented by J. Proud [27], [28] and shown in Fig. 9(a), is simply a cascade of TLs, with each line $1/2$ wavelength in length, equal in impedance, and separated by switches. The lines are alternately charged to $+V$ and $-V$, with

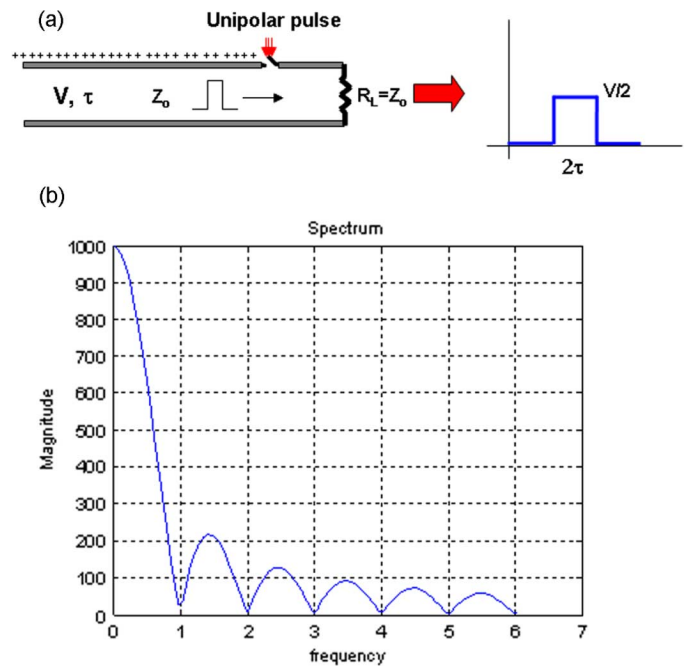


Fig. 7. (a) A charged transmission line discharged into a matched load generated a unipolar pulse at half the charge voltage and a duration equal to the double-transit-time of the charged line. (b) Frequency spectrum of a 1 ns unipolar pulse.

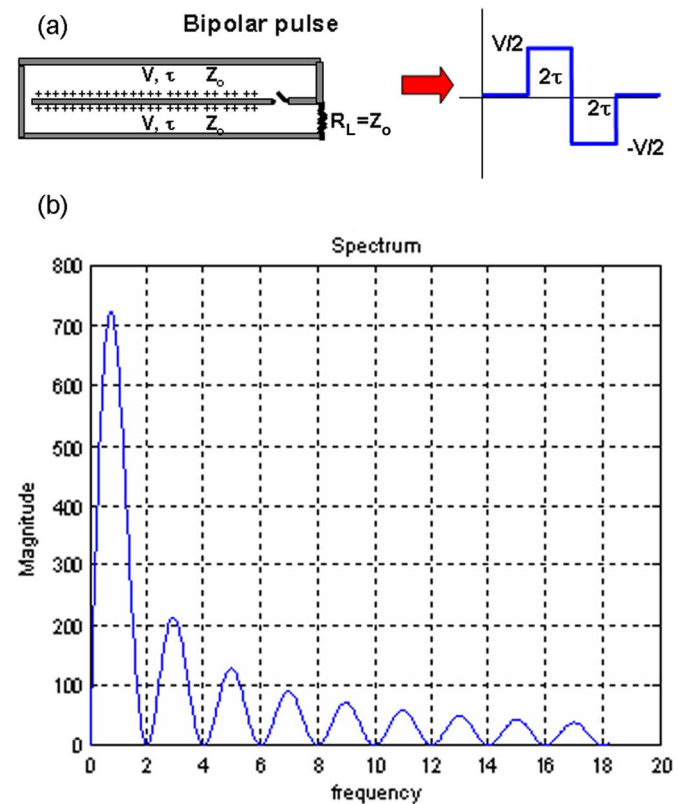


Fig. 8. (a) A charged TL design that, when switched, generates a bipolar square pulse. (b) Frequency spectrum of a 1 ns bipolar pulse ($\tau = 0.25$ ns).

all of the switches triggered at the same time. The number of half-cycles generated is twice the number of transmission lines. In theory, with lossless switches and TLs, the total pulse energy

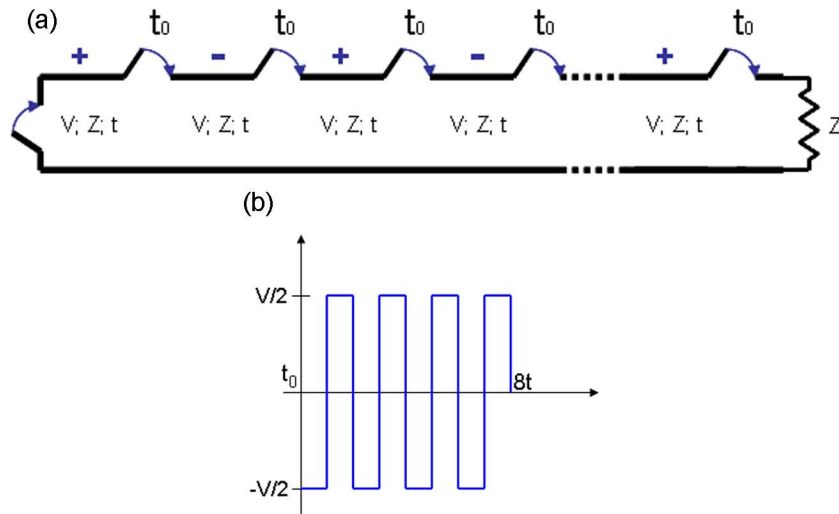


Fig. 9. (a) Schematic of frozen wave generator. (b) Representation of typical waveform for a frozen wave generator.

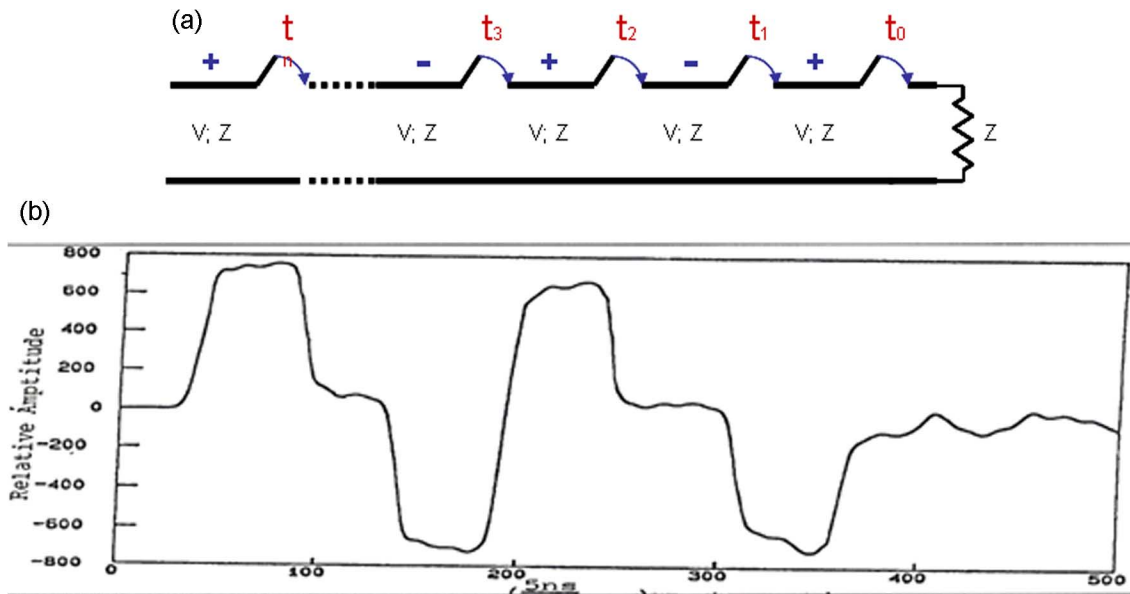


Fig. 10. (a) Schematic of sequential switched generator. (b) Experimental results showing varied delays using a sequential switch generator.

initially stored in the lines is increased by the number of lines in cascade.

A similar circuit, termed the sequentially switched generator [18], [19] and shown in Fig. 10(a), was invented by the author and is operated by closing one switch at a time, beginning with the switch closest to the load and allowing this line to discharge in a double transit time. While that switch remains closed, the second switch is closed and thus discharges the second line in a similar double transit time. The frequency is one-half that of the frozen wave generator for the same length of line. However, we can now vary the sequential delay between the switches to establish a controlled modulation, as seen in the data of Fig. 10. Therefore, arbitrary waves can be generated using the sequentially switched generator.

While these two circuit designs indeed increase the energy of the pulse when compared to single switch-line systems, the number of pulses that can be generated is severely limited by

the losses inherent to the closed switches and lines. The greater the number of sections in the circuit, the greater the number of switches and lines a pulse from the back of the network must traverse to reach the load. In contrast to avalanche switches, linear switches have a drop of only a few percent of the blocking voltage when switched *on*. Still, the cumulative loss rapidly puts a limit, albeit higher, on the number of sections. An experiment [16] using a 16-switch sequentially switched circuit (see Fig. 11) shows that the last pulse is attenuated by a factor of 2, with a corresponding energy reduction by a factor of 4. Therefore, 10 sections are about the practical limit of these circuits.

C. Advanced Circuit Configuration

Some HPM applications require both high power and high energy. Therefore, it is desirable to create circuits capable of many more TLs and switches without a reduction in energy or power. To overcome the resistive loss due to switches seen in

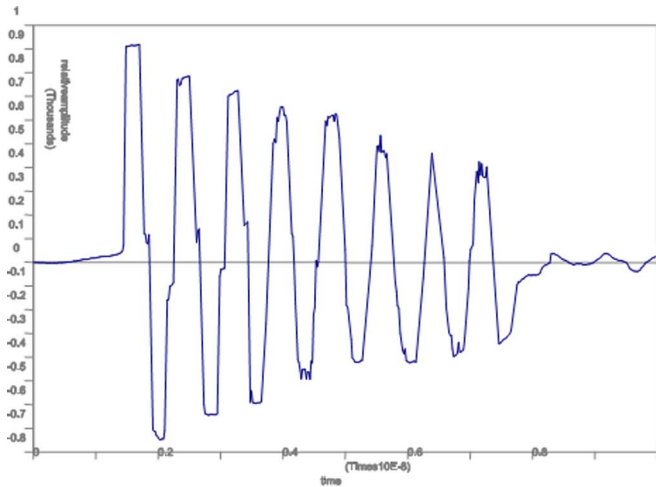


Fig. 11. 16-switch sequential switching generator [16].

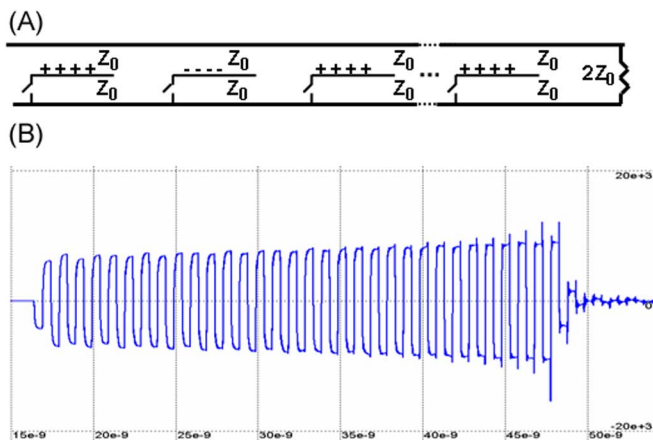


Fig. 12. (a) Conceptual diagram of an SBS circuit. (b) Modeling results for SBS circuit with 66 switch sections.

the previous designs, we present a new approach—the Switch Bypass Source (SBS) circuit, shown in Fig. 12 [29].

The SBS circuit is composed of two continuous transmission line plates which are connected to the load. Between the plates are quarter-wave-long plates forming upper and lower TLs, which are alternately charged $+V$ and $-V$, respectively, and with shorting switches at the back of each connected to the bottom plate. (The switches can also be connected alternatively to the bottom and top plates if the charge voltage is not alternating. This configuration lends itself to folding the entire circuit like an accordion.) In this system, the first switch closed is that which is farthest from the load (as opposed to the Sequentially Switched Generator). The pulse is produced in Blumlein fashion, with the pulse traveling to the load in the upper and lower plates rather than through switches. This bypassing of all the charged lines and their still open switches on the way to the load (hence the name Switch Bypass Source) causes the reduced dissipation. This circuit was invented at ECR around 1984 and presented at a classified meeting at NRL in 1988. It had the drawback of requiring embedded switches and was thus not practical. The gridded switch (Fig. 6) invented in 1999 made the SBS circuit now practical. After the discharge of the

first charged line, the second-most distant switch from the load is closed and discharges its line. As more lines are switched, each at double transit time, the energy moves forward toward the load. We observe that except for the first line, the subsequent lines do partially discharge backwards. However, as the number of sections is increased, the pulse train becomes much more uniform. The reason for this is that the majority of switching operations are in “active circuits,” where waves enter already charged or partially charged lines and the impedance matching is altered by the relative voltages encountered [30], [31]. While the signal is initially distorted by the reflections created at each section, the cumulative effect on the signal as more sections are switched is that the pulse in fact becomes very stable with a constant amplitude [see Fig. 12(b)]. In this design, the number of switches that can be operated is substantially larger than in the frozen wave or sequentially-switched TL circuits because adding switches does not increase switch losses, only copper losses due to the increased length of the circuit. It is important to note that the modeling in Fig. 12(b) includes all realistic switch losses, TL line losses, and switch inductances. We observe that the pulses are largest at the end of the pulse where the switched lines are closest to the load. High frequency spiking has been cancelled out by the various switch inductances at the beginning of the pulse, but not at the end where the pulse is closest to the load and thus encounters only one switch inductance.

The SBS circuit above does extend the number of half cycles (stages) from around a dozen for low-impedance frozen wave or sequential switching circuits to between 50 and 100 half cycles. At this point, conduction losses in the outer electrodes become large enough due to the extended length of the circuit. As was described in Section II-D on circuit theory, the ratio of $2\pi\delta/d$ defines the losses in a TL of a length of one wavelength. If the spacing, d , increases in order to allow a larger number of sections and thus cycles, the result is the reduction in peak power. An increase in the overall energy per pulse still further is accomplished by using the “unbalanced” SBS circuit shown in Fig. 13(a) [32].

In this circuit, we increase the separation between the transmission line plates to reduce the copper losses. We now alter the placement of the quarter-wave-plates such that the spacing to the bottom plate is still in the mil regime in order to provide high electric field and thus energy storage and power. While the larger separation to the upper plate stores little energy, the overall energy storage reduction is only a factor of 2. To the first order, if the upper plate separation has been increased by a factor of 10, the copper losses in the outer plate have also been reduced by a factor of 10. With this arrangement we can now accommodate a 10 fold number of sections and thus increase the overall pulse length and energy by a similar amount.

We notice, however, that there is now a much larger mismatch between individual TL than in the previous, “balanced SBS design.” Here again the interaction between the pulses are those of an active circuit where the waves enter lines with other waves already present. The sequential switching continuously enforces this resonance phenomenon. A sensitivity analysis was performed to prove that this circuit is quite robust to minor variations in timing and parameter values. Fig. 13(b) shows the modeling of an unbalance SBS circuit at 1 GHz with 528 switches

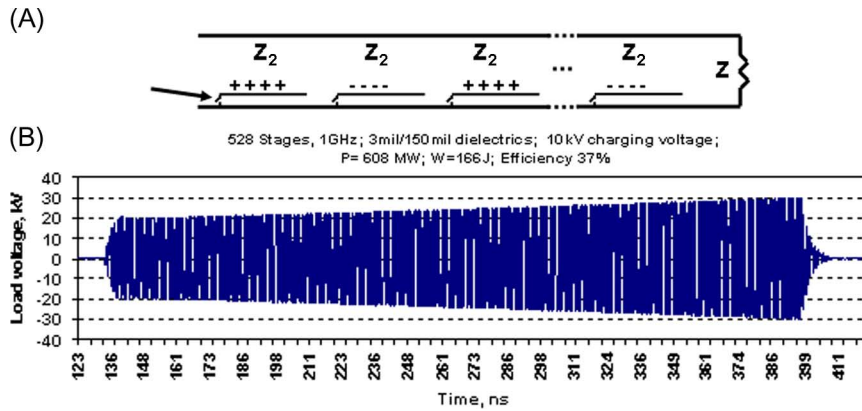


Fig. 13. (a) Conceptual diagram of an “unbalanced” SBS circuit. (b) Modeling results for a 528-stage unbalanced SBS pulse generator.

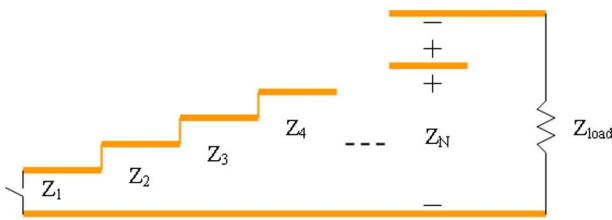


Fig. 14. A Darlington-type impedance transformer.

and sections. Again, all switch and copper losses as well as switch inductances are included. The generated power was 608 MW per meter TL width, with 166 J output energy and 37% efficiency. Overall, the unbalanced SBS circuit allows for high-power and high energy pulses that previous circuit designs could not.

D. Bipolar Pulse Integrated Transformer Circuitry

The bipolar pulse generator of Fig. 8 is operating at impedance corresponding to a thin film TL separation of about 2 mils, or 50 μm. Such a 10 cm wide line of this thickness has a characteristic impedance $Z \sim 0.1 \Omega$ and therefore transformation to a suitable radiator is required. If the generated pulse is at a frequency of 1 GHz, the pulse will radiate efficiently if the plate separation is larger than 1/4 wavelength, or ~7 cm. This is a difference in plate separation of a factor of ~1500, which is also the same order of required impedance transformation. S. Darlington [33] has shown that the charging of stepped quarter-wave-long TLs with specific increasing step impedances upon switching will generate a perfect *unipolar* (positive or negative) pulse which contains the entire charged energy (Fig. 14). The impedances of the successive line’s steps obey the relation

$$Z_i = Z_{i-1} \frac{i+1}{i-1}, \quad i = 2, 3, 4 \dots N, \quad Z_1 = 1. \quad (8)$$

S. London [34] has invented a similar stepped-line structure, but one that generates a *bipolar* pulse similar to that of the circuit in Fig. 8 but with substantial impedance transformation. The impedances of the successive line’s steps obey the relation

$$Z_i = Z_{i-1} \frac{i+3}{i-1}, \quad i = 2, 3, 4 \dots N, \quad Z_1 = 1. \quad (9)$$

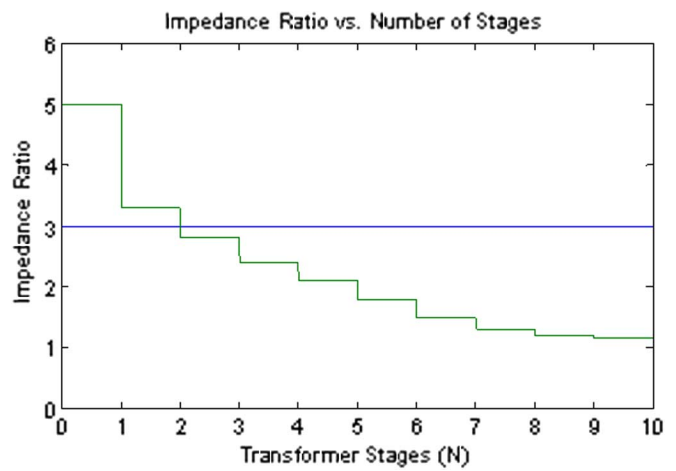


Fig. 15. An example of a sequential impedance transformer where the impedance ratio, R , at each stage varies, compared to an exponential transformer where each impedance ratio remains constant at $R = 3$.

Both the Darlington and London variants have large transformation ratios in the first few steps, while the transformation ratio of the later stages drops precipitously in order to maintain the pulse shape. For larger final transformation ratios an exponential (constant impedance multiplier between steps) setup may be used after the first few stages to increase the impedance multiplier while sacrificing minimal energy in the generated pulse. Fig. 15 shows the results of two design methodologies: i) an exponential ratio (straight line at ratio $R = 3$); ii) a Darlington/London design, where initial impedance ratio begins high at a value of five, but is reduced in successive stages and slowly diminishes. Thus, the Darlington/London design is good for transformation ratios of up to a few hundred while the exponential design is good for transformation ratios of more than a thousand depending on the acceptable pulse deterioration. Circuit and pulse design constraints will thus determine which design is appropriate for a given application.

As an example, we consider a radiator design that operates at 1/3 the air breakdown limit of HPM (10 Gw/m²), i.e., ~ 3 Gw/m². An aperture of 10 cm by 10 cm will need to radiate 30 MW, which corresponds to 3 MW/cm power per unit TL width. The transformation ratio in air from 3 mils of Kapton to the 10 cm aperture is 2400. In order to achieve this transformation

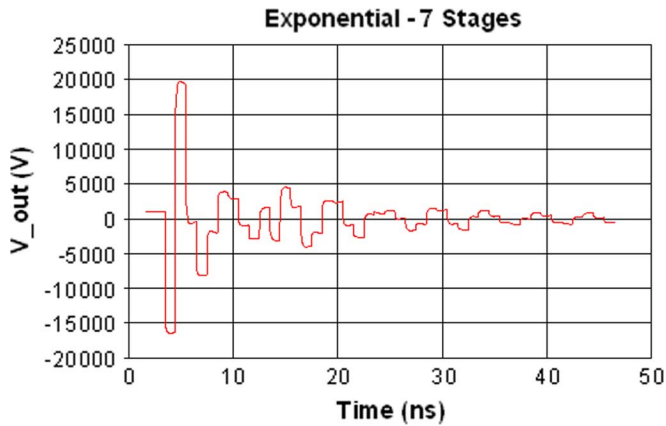


Fig. 16. The generated pulse for an exponential transformer of $R = 3.04$ for seven stages.

ratio of 2400, an exponential transformer with an impedance ratio $R = 3.04$ would require a minimum of seven stages. The generated bipolar pulse for such a system is shown in Fig. 16.

IV. RADIATION

Radiators for HPM systems have unique requirements that are not present in most other radar electronic warfare and communication systems. First, when the active antenna is operated near the air breakdown limit, as is often the case for HPM, it is impractical to illuminate a surface from a smaller area waveguide. This is due to the fact that at the waveguide, the air breakdown limit will be exceeded, which would require a special environment such as pressurized gas. Second, with large electric fields, conducting boundaries have to be controlled so as to prevent field enhancements. This must be accomplished without increasing the overall antenna area in relation to the effective area. Lastly, if the radiated power is to substantially exceed 10 GW (the typical limit of a single resonant cavity source), then the conventional solution is inherently that of many amplifiers coherently driven by a single source.

The photoconductive switch-based sources discussed in this paper provide the necessary properties to meet the requirements for an HPM radiator. The PC switches are illuminated with a single laser, which is subsequently fanned out to optical amplifiers before being introduced into the individual source switches, thus satisfying the first and third requirements as stated above. Here, an array of sources, rather than amplifiers, is operated coherently. In order to increase the Poynting vector at the aperture, and at the same time simplify the combining of the power from the individual sources, it is ideal to utilize TEM antennas. The size and spacing of the plates must take into consideration not only the power density and radiation efficiency, but also field enhancement effects.

All of the sources and the corresponding analysis in this paper dealt with parallel plate, thin film TLs. While the Poynting power in the dielectric thin film is many orders greater than air breakdown, we do not want each source aperture to necessarily open up to make an efficient radiator. Rather, it is the ensemble of apertures that need to be an efficient radiator. The goal is to radiate efficiently while still retaining a high-power density.

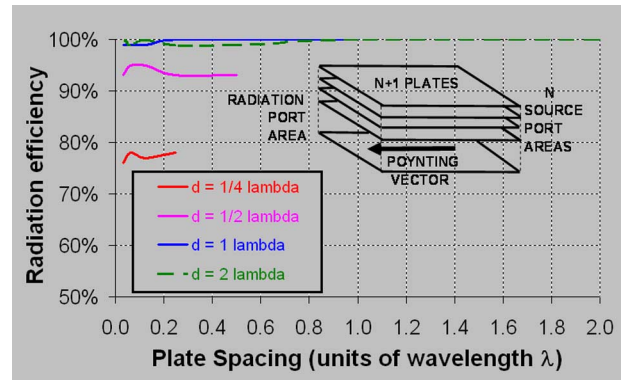


Fig. 17. Radiation efficiency of a stack of TLs as a function of individual plate spacing for various stack heights.

An HFSS analysis of the radiation efficiency of a parallel plate ensemble was performed where the ensemble thickness normalized to the wavelength varies from much less than one to values greater than one. The individual spacing between plates varies down to numbers much smaller than one, i.e., the regime where individually they will make poor radiators. As shown in Fig. 17, radiation efficiency is independent of the individual plate spacing so long as the ensemble thickness remains large relative to the wavelength. This is due to the strong coupling between cavities associated with TEM radiators. Accordingly, the various sources described in the paper lend themselves well to be stacked into radiators that operate close to the air breakdown. Therefore, the system can be scaled to arbitrarily high power by simply adding more individual units.

V. CONCLUSION

This paper describes a pathway to HPM systems at orders of magnitude higher power than present approaches can reach. It demonstrates the advantages of arraying multiple sources which utilize photoconductive switches and thin film TLs. We have further shown how this basic technology can be used in circuits. First, these configurations generate the appropriate signals for efficient radiation. Second, we have proposed unique circuits for the simultaneous generation and impedance transformation required to overcome the inherent impedance mismatch. Finally, we have shown a new family of circuits for extending the pulse train length into the hundreds of nanoseconds, thus increasing the energy without sacrificing peak power. This translates into many kilojoules per square meter on the antenna and approaching MJs and TWs for large systems whose antenna area is a few hundred square meters.

ACKNOWLEDGMENT

The author is indebted to his colleagues at BAE Systems who helped with the editing, calculations and the generation of the various figures and drawings, including S. London, J. McGeehan, D. MacLennan, C. Novotny, G. Rodriguez, and Y.-M. Sheu.

REFERENCES

- [1] D. J. Page, "Some advances in high power, high dI/dt, semiconductor switches," in *Proc. Int. Conf. Energy Storage, Compression, and Switching*, Nov. 1974, p. 415.

- [2] D. J. Pages and J. S. Roberts, "Light activated thyristor with high di/dt capability," U.S. patent 3 893 153, Jul. 1, 1975.
- [3] D. H. Auston, "Picosecond optoelectronic switching and gating in silicon," *Appl. Phys. Lett.*, vol. 26, pp. 101–103, 1975.
- [4] O. S. Zucker, J. R. Long, V. L. Smith, D. J. Page, and J. S. Roberts, "Nanosecond switching of high power laser activated silicon switches," in *Proc. Int. Topical Conf. Electron Beam Research and Technology*, Albuquerque, NM, Nov. 3–5, 1975, pp. 538–552, [see also, Lawrence Livermore laboratory report UCRL-77449 (November 1975)].
- [5] J. Long and O. Zucker, "Edge illuminated laser activated silicon switch," U.S. Atomic Energy Commission, Record of Invention, AEC Case No. IL-6175, Oct. 23, 1975.
- [6] P. LeFur and D. H. Auston, "A kilovolt picosecond optoelectronic switch and Pockel's cell," *Appl. Phys. Lett.*, vol. 28, p. 21, 1976.
- [7] O. Zucker, "Laser activated and sustained silicon transistor," U.S. Atomic Energy Commission, Record of Invention, AEC Case No. IL-6174, Feb. 3, 1976.
- [8] O. S. F. Zucker, J. R. Long, V. L. Smith, D. J. Page, and P. L. Hower, "Experimental demonstration of high-power fast-rise-time switching in silicon junction semiconductors," *Appl. Phys. Lett.*, vol. 29, pp. 261–263, 1976.
- [9] J. Long and O. Zucker, "New experiment with light activated silicon switches," Lawrence Livermore Lab., Report UCRL-80492, Dec. 27, 1977.
- [10] C. H. Lee, "Picosecond optoelectronic switching in GaAs," *Appl. Phys. Lett.*, vol. 30, pp. 84–86, 1977.
- [11] K. H. Schoenbach, J. S. Kenney, F. E. Peterkin, and R. J. Allen, "Temporal development of electric field structures in photoconductive GaAs switches," *Appl. Phys. Lett.*, vol. 63, pp. 2100–2102, 1993.
- [12] D. C. Stoudt, M. A. Richardson, D. L. Demske, R. A. Roush, and K. W. Eure, "High-power subnanosecond operation of a stable optically controlled semiconductor switch (BOSS)," in *1994 IEEE Int. Conf. Plasma Science Conf. Rec.*, Jun. 6–8, 1994, pp. 191–192.
- [13] G. Mourou and W. Knox, "High-power switching with picosecond precision," *Appl. Phys. Lett.*, vol. 35, no. 7, p. 492, 1979.
- [14] L. Bovino, T. Burke, B. Youmans, M. Weiner, and J. Carter, "Recent advances in optically controlled bulk semiconductor," in *Proc. 5th IEEE Pulsed Power Conf.*, Arlington, VA, 1985, pp. 242–245.
- [15] W. C. Nunnally, "Photoconductive pulse power switches: A review," in *Proc. 5th IEEE Int. Pulsed Power Conf.*, Arlington, VA, 1985, pp. 235–241.
- [16] D. M. Giorgi, A. H. Griffin, D. E. Hargis, A. McIntyre, and O. S. F. Zucker, "High power, light activated switching: Experiment and applications," in *Proc. 8th IEEE Int. Pulsed Power Conf.*, Jun. 16–19, 1991, pp. 122–125.
- [17] O. S. F. Zucker, in *Department of Defense High Power Microwave Conf.*, Albuquerque, NM, 1985. (Classified).
- [18] O. S. F. Zucker and J. R. Long, "Generated and method for generating microwaves," U.S. Patent 5 109 203, Apr. 28, 1992.
- [19] O. S. F. Zucker, "Method and Apparatus for Digital Synthesis of Microwaves," US Patent 5,185,586, (Filing date: May 3, 1991; Issue Date: Feb. 9, 1993).
- [20] J. C. Martin, "Pulse breakdown of large volumes of mylar in thin sheets," Atomic Weapons Research Establishment, Mar. 30, 1967.
- [21] E. Harari, "Dielectric breakdown in electrically stressed thin films of thermal SiO₂," *J. Appl. Phys.*, vol. 49, pp. 2478–2489, 1978.
- [22] O. S. F. Zucker, I. A. McIntyre, and D. M. Giorgi, "High power light activated switching: Theory," in *Proc. 8th IEEE Int. Pulsed Power Conf.*, Jun. 16–19, 1991, pp. 126–129.
- [23] O. S. F. Zucker and I. A. McIntyre, "Light activated semiconductor switches for ultra-wideband radar," in *Introduction to Ultra-Wideband Radar Systems*. Boca Raton, FL: CRC Press, 1995.
- [24] A. H. Griffin, O. S. F. Zucker, and D. M. Giorgi, "Sequentially switched PFN for inductive and resistive loads," in *Proc. 8th IEEE Int. Pulsed Power Conf.*, Jun. 16–19, 1991, pp. 296–298.
- [25] O. S. F. Zucker, D. M. Giorgi, and I. A. McIntyre, "Non linear transmission lines using photo-dependent nonlinear capacitors," in *Proc. 8th IEEE Int. Pulsed Power Conf.*, Jun. 16–19, 1991, pp. 299–301.
- [26] O. S. F. Zucker, "Isolated control apparatus incorporating light controlled power semiconductors," U.S. patent 7 296 753, Nov. 20, 2007.
- [27] J. M. Proud, "Radio frequency generators," U.S. patent 3 484 619, Dec. 16, 1969.
- [28] J. M. Proud, Jr. and S. L. Norman, "High-frequency waveform generation using optoelectronic switching in silicon," *IEEE Trans. Microw. Theory Tech.*, vol. MTT-26, pp. 137–140, 1978.
- [29] O. Zucker, "Method and apparatus for digital synthesis of microwaves," U.S. patent 7 268 641, Sep. 11, 2007.
- [30] I. D. Smith, "A novel voltage multiplication scheme using transmission lines," in *Proc. IEEE Power Modulator Symp.*, 1982, vol. 15, pp. 223–229.
- [31] I. D. Smith, "Principles of the design of lossless tapered transmission line transformers," in *Proc. 7th Pulsed Power Conf.*, Jun. 1989, pp. 103–107.
- [32] O. Zucker and S. Y. London, "Method and apparatus for digital synthesis of long microwave pulses," U.S. Patent Application, to be submitted.
- [33] S. Darlington, "Impulse generator," U.S. patent 2 420 302, May 13, 1947.
- [34] S. London, "Bipolar pulse generators with voltage multiplication," U.S. Patent Application Publication 0165839, Jul. 19, 2007.



Oved S. F. Zucker (M'88) received the B.S. degree in electrical engineering from City College of New York (CCNY), New York, NY, in 1965.

He spent his first 12 professional years at Lawrence Livermore National Laboratories where he began his original work on HPM. While at Physics International from 1978 to 1981, he worked on pulsed power systems in both magnetics and high voltage generators. From 1981 to 1983, he worked on tokamaks for Inesco. During the period of 1983–1997, he founded the company ECR where most of the PC-switch-based HPM work took place. Here he developed the meat grinder, all-inductive pulsed power system. In 1997, he founded OZI and continued his work with PC-switch-based systems for the Fly by Light program. From 1999 to 2008, he worked for APTI, which was acquired by BAE Systems. In 2008, he co-founded Polarix Corporation, San Diego, CA.